^{14}N nuclear-quadrupole-resonance study of solitons and charge-density waves during the Peierls transition in potassium tetracyanoquinodimethane

Arturo Colligiani
Istituto di Chimica Industriale, Universitá di Messina, S. Agata, 98100 Messina, Italy

Juan Murgich*
Centro de Química, Instituto Venezolano de Investigaciones Científicas (IVIC), Apartado 21827, Caracas 1020A, Venezuela

Rocco Angelone and Roberto Ambrosetti
Istituto di Chimica Quantistica ed Energetica Molecolare del Consiglio Nazionale delle Richerche, Via Risorgimento 35, 56100 Pisa, Italy

(Received 6 July 1988; revised manuscript received 11 October 1988)

The temperature dependence of the intensity, frequency, and line shapes of the ^{14}N nuclear-quadrupole-resonance spectrum in potassium tetracyanoquinodimethane (K-TCNQ) showed that the Peierls transition consists of a complex set of transformations that on heating leads to a first-order transition at 130 °C with hysteresis. Above 130 °C, the high-temperature (HT) phase containing fluctuating charge-density waves (CDW) becomes incommensurate, transforms into a multisolitonic phase with narrow solitons above 141.5 °C, and near the decomposition temperature changes towards the single-soliton limit. On cooling from above 150 °C, K-TCNQ transforms directly from the HT multisolitonic to a HT commensurate phase at 141.4 °C that coexists with the low-temperature phase from 128 °C but only disappears below 90 °C. The previously undetected transition observed at 141.5 °C on heating and cooling is attributed to a change in the effective dimensionality in the ordering of the CDW's along the TCNQ stacks. The complex set of transitions found in the fully ionic K-TCNQ showed that the Peierls transition is likely to be a two-step process even in simple salts as predicted theoretically by Zhou and Gong [J. Phys. C **21**, L561 (1988)].

I. INTRODUCTION

The Peierls phase transition of potassium tetracyanoquinodimethane (K-TCNQ) has been studied by means of different techniques[1–7] which give, predominantly, information about bulk properties of this paramagnetic system. The existence of a single but rather simple Peierls transition has been the basic assumption in the interpretation of all these experiments. The measurements which have been performed have been carried out at temperatures slightly below and a few degrees above the assumed transition point.[1–7] In most cases, the characteristics of the two resulting phases have been independently studied[5–7] but little or no attention has been paid to what happens in the temperature range where the transition seems to occur. Some authors have described theoretically the Peierls transition found in K-TCNQ as a continuous transition[8] while others, taking into account the discontinuities in the lattice parameters, have predicted a first-order transition.[9] Terauchi[4] has studied the Peierls transition using the superlattice x-ray reflections of the low-temperature (LT) phase and the diffuse scattering related to the fluctuations in the TCNQ stacks above the transition temperature. These results have provided valuable although limited information of the microscopic changes present in K-TCNQ at the transition. On the other hand, detailed studies of the Peierls phase transition have shown that such a transformation may involve incommensurate and commensurate charge-density waves.[4] It has also been found that the precursor effects produced by the Kohn anomaly that accompanies the Peierls transition are present in many TCNQ salts.[4] It is likely that similar effects may be present in the simple and fully ionic K-TCNQ salt.

In order to investigate the structural and other changes produced by the Peierls transition in K-TCNQ, a nuclear-quadrupole-resonance (NQR) study using a Fourier-transform (FT) pulsed spectrometer has been undertaken. NQR is a very sensitive tool in the study of the variations in the charge distribution around quadrupolar nuclei[10,11] and may provide unique information about the Peierls phase transition present in K-TCNQ.

The study of the intensities and frequencies of the ^{14}N NQR spectrum with temperature in K-TCNQ shows that the changes produced in the TCNQ stack by the Peierls transition leads to a first-order transition at 130 °C with hysteresis. These results were confirmed by means of EPR measurements and by differential scanning calorimetry. On heating, the first-order transition leads to a high-temperature (HT) phase that coexists with the other phase, becomes incommensurate around 134 °C, and transforms abruptly to a previously undetected multisolitonic HT phase at 141.5°C. The multisolitonic phase changes, when approaching the decomposition temperature, towards the single-soliton limit. The variation in the CDW's observed at 141.5°C on heating and cooling has been attributed to a change in the effective dimensionality in the ordering of these waves along the

$TCNQ^-$ stacks. On cooling from above 150 °C, K-TCNQ changes abruptly from the HT multisolitonic to a HT commensurate phase that only disappears around 90 °C after coexisting with the LT phase from 128 °C. The extension of the hysteresis in K-TCNQ was found to be related to defect concentration and the amount of time allowed for recrystallization above T_c.

The complexity of the transition found in the simple and fully ionic K-TCNQ showed a parallelism with that found in partially ionic tetrathiofulvalene-tetracyanoquinodimethane (TTF-TCNQ) indicating that factors such as the interstack coupling in addition to the degree of charge transfer play an important role in determining the characteristics of the Peierls transition.

II. EXPERIMENTAL DETAILS

Measurements were taken on 5 g of the polycrystalline sample used in Ref. 11 and prepared as in Ref. 12. The sealed glass vial[13,14] was immersed in vaseline oil for measurements up to 120 °C and in silicone oil from 90 to 190 °C in a F-4391 Haake thermostat. Temperature measurements were taken using a Pt resistance calibrated at 0 and 100 °C. The nonlinearity of the Pt resistance was corrected by a quadratic fitting of ten readings between 80 and 190 °C taken against a mercury-in-glass thermometer with a 0.1 °C resolution. The thermometer readings were corrected for the emergent stem effect. The estimated standard deviation on the temperature measurements was ±0.2 °C and the resolution better than ±0.01 °C. The final run (up to 270 °C) was made in an insulated Cu furnace of thick walls where the heating and control elements were inserted.

NQR measurements were made with a FT spectrometer described previously;[14] the only change was the use of a HP 3325 A frequency synthesizer as the rf source. Since ^{14}N has spin $I=1$, two NQR lines ($\nu^+ > \nu^-$) are usually observed for each crystallographically independent N site.[10] The lines are $\nu^{\pm}=(3e^2qQ/4h)(1\pm\eta/3)$, where e^2qQ/h is the nuclear-quadrupole-coupling constant and η is the symmetry parameter of the electric field gradient[10] (EFG). For the ν^+, the pulse repetition rate was 100 sec^{-1}, with typical averaging times of 2–5 min while for the ν^- lines, 3 pulses/sec with averaging times of 30 to 60 min were used. A typical signal-to-noise ratio was greater than 200 for the ν^+ lines and considerably lower for the ν^- lines.

A requirement of the present measurements was amplitude calibration, needed in order to compare amplitudes or intensities measured under different experimental conditions. The major factors affecting the amplitude of the lines obtained with a FT pulsed spectrometer[14] were (a) the rf reference level; (b) the rf gain of the receiver and the low-frequency gain of the amplifiers in the data acquistion circuitry; (c) the pulse repetition rate; (d) the pulse length and amplitude; (e) the rf offset (rf difference between the exciting pulse and the resonance frequency); (f) the tuning of the rf circuits [especially that of the sample inductance-capacitance (LC) circuit, since the receiver and transmitter rf circuits are much less selective]; (g) a slight frequency dependence of the receiver gain; and (h) the selectivity of the post-detection low-frequency filter. The factors (a) through (d) were simply left fixed at a given setting, and factor (h) was eliminated by keeping the cutoff frequency of the filter above 100 kHz (the maximum low-frequency component in actual spectra was 40 kHz). The factors (e), (f), and (g) were taken into account and their effect suitably corrected (see Appendix A).

Differential-thermal-analysis (DTA) and Differential-scanning-calorimetry (DSC) measurements were carried out using a model 990 Dupont thermal analyzer. The best results were obtained with the DSC technique at a heating rate of 10 °C/min and a sample weight of around 100 mg. For the EPR measurements, a Varian E-122 spectrometer equipped with a rectangular cavity for the X-band and magnetic modulation was used. The temperature was measured with a thermocouple located inside the Dewar containing the cavity with the sample.

III. EXPERIMENTAL RESULTS

The ^{14}N spin-lattice relaxation time T_1 was rather constant with temperature and estimated to be between 0.5 and 1 msec. A more precise measurement was not possible because the pulse separation[13] could not be reduced to the limits required for an accurate determination of such a short T_1. Measurements on the ν^- lines, on the other hand, had the additional difficulty of their low intensity; however, the T_1 values were found to be around 100±20 msec.

Similar results in the temperature dependence of the intensities were obtained on both sets of lines; however, due to their greater ease of observation, quantitative measurements were made on the ν^+ lines only. The amplitude measurements were made so that at least one was obtained on either side of the spectrum. Resonance frequencies were reproducible to within 50 Hz while the corrected amplitudes had a residual standard deviation of less than 10%. The measurements were taken in five different temperature cycles: an "initial" cycle, in which the hysteresis was found, and a "second" cycle, in which measurements were taken over the range 30–90 °C just to have continuity with previous measurements.[11] In the next cycle (the "160" cycle), the temperature followed gradually and monotonically the sequence 90–163–90 °C, while in the "190" cycle, the temperature was raised rapidly from 90 to 190 °C, then decreased slowly back to 90 °C. In both the 160 and 190 cycles the starting temperature was 23 °C. In the "final" cycle, the decomposition temperature of the sample was attained.

The behavior of the spectrum on heating was quite reproducible, provided the sample was kept a few minutes around room temperature. At that temperature and up to 128 °C, the sample showed the known eight ν^+ and eight ν^- lines (see Figs. 1 and 2), of the LT phase[11] (labeled a through h). Above 128 °C, weak additional lines appeared [Figs. 3 and 4(c)], which grew rapidly in amplitude as the temperature was raised. After each temperature change, the new amplitude of the lines appeared to be steady following a short time (2–5 min) required for thermal stabilization. No time effects on the spectrum was seen even after two full days, at any tem-

perature, except in extreme cases (such as cooling from 160 to 100 °C in less than 10 min). The overall thermal history of the line amplitudes for the two 160 and 190 cycles is reported in Fig. 3. When the temperature reached 130 °C and above, the high-temperature (HT) ν^+ lines [Fig. 4(c)] grew rapidly in amplitude, tending to plateau above 140 °C. Over the same range, the low-temperature (LT) lines decreased accordingly [Fig. 4(e)]. At 141.5 °C, the spectrum changed rather abruptly. Most of the LT lines disappeared entirely above that temperature as seen in Fig. 4(g). Nevertheless, at about 130 °C, the intensity of the two *b* and *g* LT ν^+ lines became constant and started to be part of the now convoluted HT lines[15] [Fig. 4(e)]. In general, the ν^- lines behaved in a very similar manner as is seen in Fig. 5. Above 141.5 °C, each of the HT lines showed a pair of edges or satellite (*s*) lines that on further heating decreased in amplitude. The behavior described so far is quite reproducible, provided that the sample was kept around room temperature for a few minutes.

The discontinuities in frequency found between the LT and HT phase showed the existence of a first-order transition.[10] The noticeable changes in the line shapes found at 141.5 °C on heating also suggested the existence of another previously undetected transition.

The behavior on cooling depends on the temperature at which it starts. In general, on cooling from above 142 °C, a further increase in amplitude for the HT lines was observed, with a parallel increase for the edge or *s* lines [Figs. 3 and 4(h)]. Below 141.5 °C, the *s* lines disappeared abruptly and the spectrum was composed only by two strong HT lines, provided that the starting temperature was high enough [Fig. 4(f)]. In fact, the LT lines may be seen to appear in the spectrum just below 141.5 °C when the maximum temperature had been moderately higher than, say 150 °C. Nevertheless, if the maximum temperature had been higher, say 190 °C, the *s* lines would have been extremely weak and the LT lines undetectable. In a specific cooling process starting at 190 °C and just below 141.5 °C, one finds a spectrum formed by only two intense HT lines [Fig. 4(d)] that did not change their amplitude appreciably over a range of almost 10 °C. Only below 133 °C, weak LT lines began to increase in intensity rapidly on cooling [Fig. 4(b)], while the HT lines started to decrease only around 122 °C as seen in Fig. 3. Nevertheless, at that temperature, on heating from room temperature, the HT lines could not be seen at all [Fig. 4(a)]. It is just the extent of the hysteresis, measured as the difference in the line amplitudes between heating and cooling process at some temperature, that depends strongly on the thermal history of the K-TCNQ sample. The resonance frequency of all detectable lines, however, was found to be entirely independent of the thermal history.

In the "final" high-temperature run (up to 270 °C), we

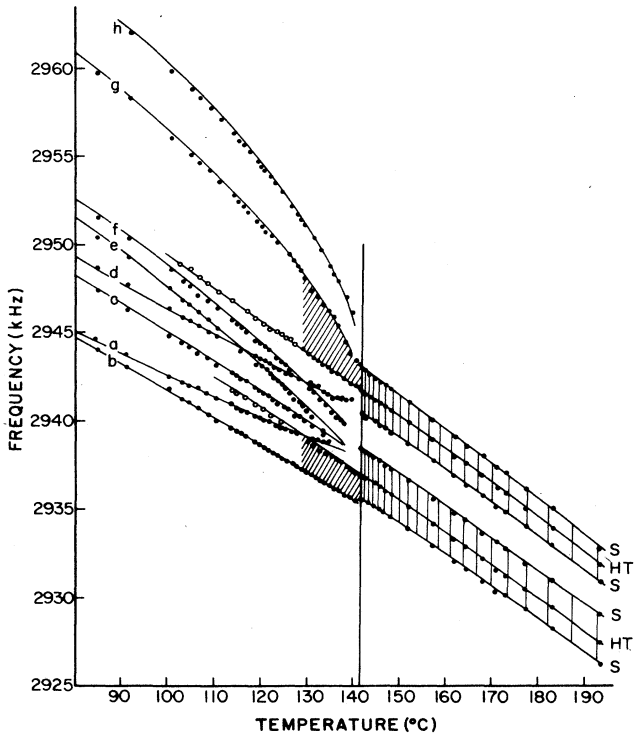

FIG. 1. Temperature dependence of the ν^+ lines of K-TCNQ. The solid circles correspond to the ν^+ lines obtained on heating and cooling. The open circles represent the ν^+ lines of the HT phase obtained on cooling at temperatures where these lines were not observed on heating. The shadowed areas correspond to the temperature intervals where incommensurate phases were observed.

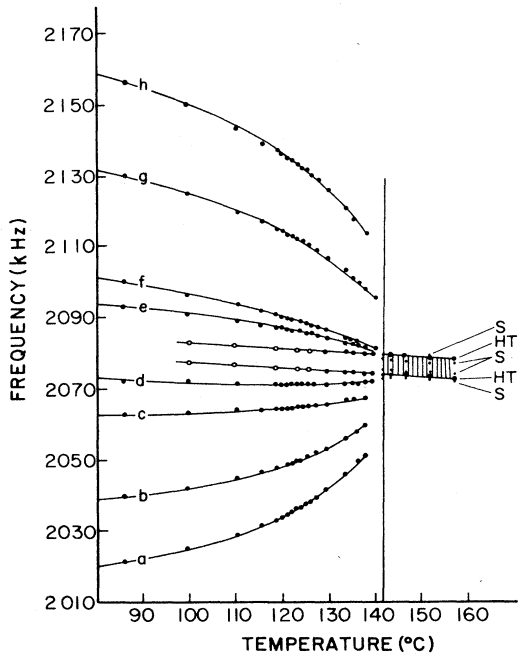

FIG. 2. Temperature dependence of the ν^- lines of K-TCNQ. The solid circles correspond to the ν^- lines obtained on heating and cooling. The open circles represent the ν^- lines of the HT phase obtained on cooling at temperatures where these lines were not observed on heating. The shadowed area corresponds to the temperature interval where incommensurate phases were observed.

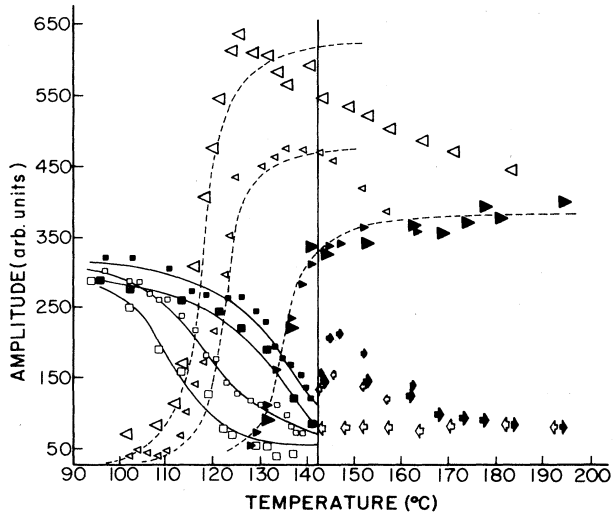

FIG. 3. Temperature dependence of the corrected intensities of the ν^+ lines of the ^{14}N NQR spectrum of K-TCNQ. The sum of the intensity of all the ν^+ lines was used in the plot. The small (large) triangles and squares correspond to the 160 (190) cycle. The small (large) arrows represent the s edge intensities observed in the 160 (190) cycle. The dashed and solid lines were drawn as visual aids only.

found that the frequency dependence above the transition was linear with temperature and that the HT lines broadened slightly while the edge lines steadly decreased its intensity. About 10° below the decomposition temperature the edge lines disappeared in the noise.

Differential scanning calorimetry (DSC) measurements performed by heating the sample have given clear evidence that a complex set of transitions exists in K-TCNQ. A noticeable amount of heat began to be absorbed at 134 °C while a second and previously undetected absorption was observed at about 142 °C (see Fig. 6). The two absorptions produced rather broad peaks which were, nevertheless, easily distinguishable and which could be well reproduced on many repeated measurements. The broad peaks observed in K-TCNQ are indicative of rate-controlled transitions such as first-order transformations. Unfortunately, no similar data were obtained when the temperature was lowered because the thermal analyzer did not have a controlled cooling system.

The measurements of the variation of the EPR line intensity with temperature are shown in Fig. 7. Because the line shape did not change much, the line intensity is expected to be proportional to the paramagnetic susceptibility.[1] If the sharp variation on the inflection of the curve is interpreted as the point where a phase transition occurs[1] then a hysteresis of around 20 °C exists in the K-TCNQ used in this work.

IV. DISCUSSION

A. FT-NQR study of a first-order phase transition

NQR provides a microscopic probe and thereby makes possible investigations of local aspects associated with phase transitions.[16] The resonant frequencies are determined by the Hamiltonian[10] $H_Q = -\overleftrightarrow{Q}:\overleftrightarrow{\nabla E}$, where $\overleftrightarrow{Q}$ is the nuclear quadrupole moment tensor and $\overleftrightarrow{\nabla E}$ is the EFG tensor at the nuclear site. When a phase transition is accompanied by alterations in the local EFG, the resonance lines are split or displaced[16] and the order of the transition is obtained from the continuity or discontinuity of the NQR frequencies at the transition temperature.[10,16] Second-order transitions produce a continuous change and/or splitting in the frequencies while in the first-order transitions discontinuities are found at the transition temperature.[10,16] The changes observed in the DSC data, in the EPR line, and in the shape, intensity, and frequency of the NQR lines with temperature showed that a rather complex set of transitions occurs in K-TCNQ contrary to early findings.[1-5] The hysteresis found in the intensity of the N lines showed that beside the incipient second-order transformation[5] there is another that proceeds by nucleation and growth. The intensity of superlattice x-ray reflections[4] related to the displacements of the TCNQ molecules exhibited a gradual and considerable decrease from 30 to 120 °C. Nevertheless, at the latter temperature, a weak but discontinuous drop in intensity was encountered indicating that the structure varies continuously over a wide temperature range until a first-order transition occurs.[4] In this type of transition, the HT phase cannot be obtained by continuously varying the position and/or orientation of molecules and atoms of the LT phase. In that case, a boundary or wall delineates the nuclei of the HT phase from the surrounding matrix.[17] The required nucleation for the transition occurs only above the equilibrium temperature, where both phases coexist (T_0), and if a suitable density of defects is present in the crystals.[17] The transition temperature and the orientation of the daughter crystal is precoded in each type of active defect. So, in a polycrystalline sample, each of the single microcrystals shows a different transition temperature because, in general, the activation energies of the defects cover a rather wide spectrum of values.[17] Upon heating (or cooling), the transition in the microcrystals takes place at different times, extending the transformation over a noticeable temperature range. Also, at each temperature within that range, a mixture of the two phases coexists. If the heating is slow enough, the relative quantity of the phases does not depend on the rate of heating.[17] These results explain the simultaneous detection of the HT and LT lines of K-TCNQ with no appreciable change of the intensity with time after thermal equilibrium within the transition range has been reached.

The transition temperature of a first-order transformation is defined as that corresponding to the maximum rate of change of the phase ratio with temperature.[17] Nevertheless, such a temperature is shifted with respect to T_0 by no less than a threshold value that depends strongly on the active defects present in the sample.[17] Because the initial defect concentration is determined by the crystal growth process and impurities,[17,18] then samples obtained by rapid recrystallization as in this work and by slow diffusion[1-5] will exhibit quite diverse concentrations of nucleation centers. This fact plus the effect

of the different thermal treatments employed in each case explains the difference between the reported[1–5] values of T_c and those obtained in the present work.

Figure 3 shows that the intensity of the HT lines increases when the temperature is lowered toward T_c. Such a behavior could be explained by the recovery and recrystallization process[18] that occurs in plastically deformed or strained crystals. The strained regions produced by the first-order transition[17,18] will generate a spread of the EFG values shifting the frequency of the affected nuclei away from the resonance lines of the unperturbed portion of the grains.[19] The recrystallization

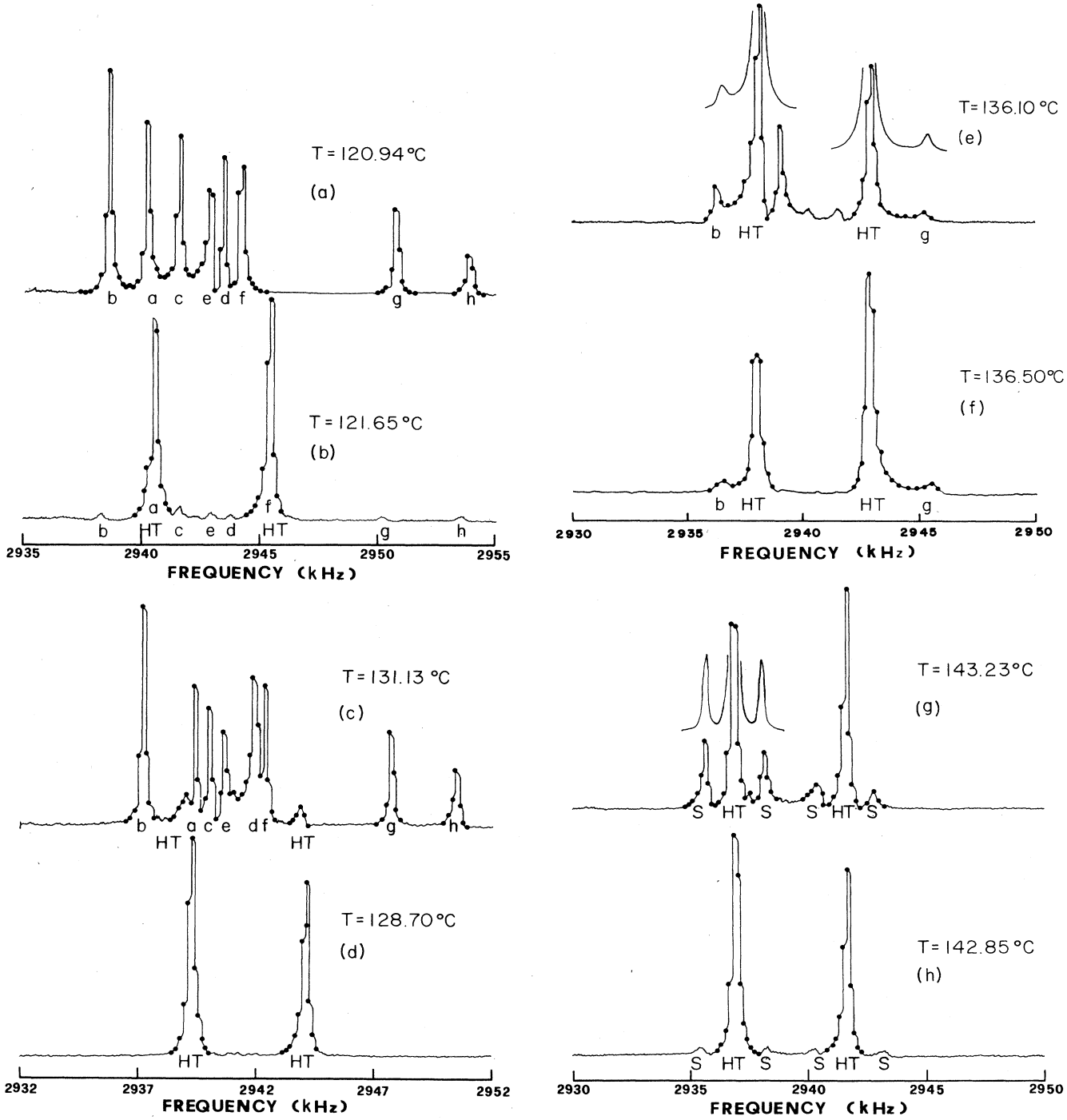

FIG. 4. FT spectrum of the ν^+ lines of K-TCNQ observed at different temperatures. Parts (a), (c), (e), and (g) were observed on heating while parts (b), (d), (f), and (h) correspond to the same lines but obtained on cooling. Also in part (e) is shown the simulated line shape that gave for the low-frequency line $p=2$, $\Delta=0.08$, $\phi_0=90°$ while for the other line $p=2$, $\Delta=0.01$, $\phi_0=0°$.

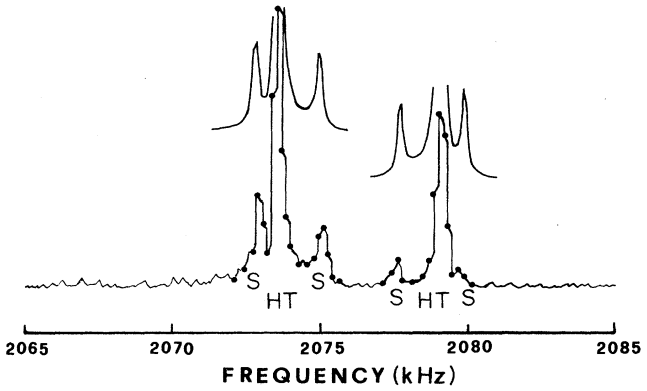

FIG. 5. FT spectrum of the ν^- lines of K-TCNQ observed at 150 °C on heating. Also is shown the simulated line shape that gave for this line $p=2$, $\Delta=0.005$, $\phi_0=33°$.

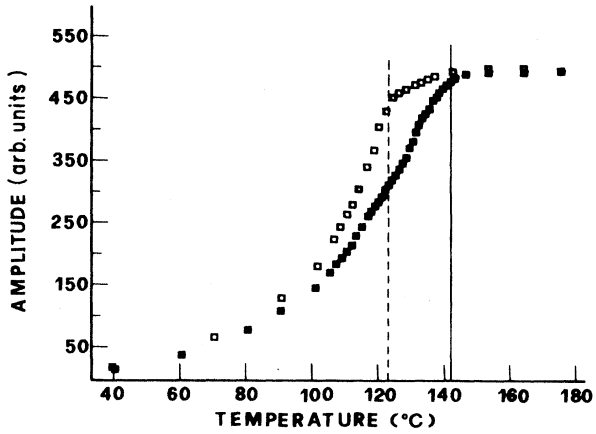

FIG. 7. Temperature dependence of the intensity of the EPR line observed in K-TCNQ showing the hysteresis effect found in this material.

process[18] induces a growth that generates large grains free from strains therefore increasing the intensity of the observed lines by augmenting the number of unperturbed nuclei. On the other hand, the increase in intensity is more marked in the 190 (~50%) than in the 160 cycle (~30%) as seen in Fig. 3. In the 190 cycle a much larger time was spent above T_c so an extensive recrystallization process[18] took place and a large increase in intensity was observed. In the 160 cycle, on the other hand, a shorter time was available and therefore a smaller increase in intensity was obtained.

The recrystallization process[18] in K-TCNQ will also increase the extension of the hysteresis through the resulting depletion of nucleation centers. Microwave conductivity measurements[20] showed that repeated passes through the transition region decreased the defect concentration in K-TCNQ. As many hours are needed to perform the NQR measurements, a noticeable degree of recrystallization is produced in each cycle. Therefore, the extension of the hysteresis determined with that technique will be influenced by the depletion of nucleation centers that necessarily occurs in each cycle. This was confirmed by the fact that the hysteresis found in the 190 cycle was larger by almost 10° than in the 160 cycle as seen in Fig. 3. The differences in the initial defect concentration and the different thermal treatments employed in each case also explain the scatter found in the extension of the hysteresis determined by x-rays[4,5] and by the present NQR and EPR measurements.

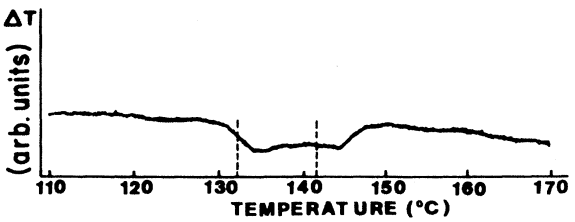

FIG. 6. Typical differential scanning calorimetry curve obtained in K-TCNQ.

B. Peierls (or spin-Peierls) transitions

The variations in the intensity of the NQR lines and the discontinuity observed in the frequencies showed that there is a weak but clearly discernible first-order phase transition in K-TCNQ with hysteresis.[16] Such a phase transition is expected to be driven by the softening of phonons related to a Peierls transition.[21] Peierls[22] showed that the electron-phonon interaction produces a charge-density wave (CDW) in a one-dimensional electron gas. The CDW, in turn, creates a periodic potential in the lattice which causes a distortion of wave vector $2k_F$, where k_F is the Fermi wave vector. Above T_c, the phonon system reflects the impending transition in the damping for wave vectors[21] near $2k_F$. A dip in the phonon-energy spectrum is generated at that wave vector that is known as the Kohn anomaly.[21] As the temperature is lowered towards T_c, the dip at $2k_F$ lowers until $\omega_k=0$ at $2k_F$ producing the Peierls distortion.[22] For the anisotropic salts of TCNQ that transition results in a distortion that leads to the static dimerization of the TCNQ stacks below[21] T_c.

In compounds where the spin-Peierls transition occurs, the electrons are well localized and the spins are coupled to the phonons and between themselves through an antiferromagnetic interaction.[23] The magnetoelastic coupling through spin-density waves (SDW) thus produced is responsible for the spin-Peierls phase transition that will generate also a dimerization in the TCNQ columns.[23]

The properties of K-TCNQ were interpreted by means of a one-dimensional Hubbard-Heisenberg Hamiltonian.[8,9] Assuming the existence of a spin-Peierls transition, Takaoka and Motizuki[9] predicted a first-order transition by considering that the spin-phonon interaction is caused by the modulation of the exchange interaction due to the lattice distortions. Nevertheless, Jacobs and co-workers[23] concluded that K-TCNQ is an intermediate case between the regular Peierls and the spin-Peierls transition because the Coulomb energy of a doubly occupied TCNQ may be

not as high as previously assumed[8,9] for that complex. Experimental studies[24] indicate that K-TCNQ is in the intermediate-coupling limit where CDW's and SDW's may coexist.[21] In a CDW, the electron density is not uniform but has a periodic modulation,[21] producing changes in the EFG components that modifies the shapes and frequencies of the regular lines.[15,25,26] In a SDW the lines will be affected by the modulation in the spin density only if the charge distribution around the nuclei is changed. In K-TCNQ, where there is one unpaired electron per TCNQ molecule,[11] the SDW in the ground state will correspond only to an alternation of the spins of the extra electron along the stacks[21] so no direct contribution to the EFG is expected in this case. Nevertheless, in a spin-Peierls transition, the magnetoelastic coupling will dimerize the TCNQ stacks[23] thus affecting the EFG through the resulting charge modulation. Therefore, the NQR data obtained in compounds undergoing Peierls transitions will provide information about the resulting charge modulation but not about the type of wave causing that perturbation.

In K-TCNQ, the Peierls transition starts high above T_c as a dynamical distortion (or fluctuating CDW) involving local dimerization of the TCNQ stacks that has a finite coherence length and correlation time. A coherence length of only a few lattice constants could be found as a result of the existence of a Kohn anomaly[27] at that temperature. As an example of this effect, in Na-TCNQ a coherence length of about ten molecules was found at T_c+23 °C along the chain and only one molecule in a direction perpendicular to the stack.[4] A progressive increase of transverse order of the CDW's is expected on cooling with little or no correlation between the phase in the chain direction.[27] As the temperature is lowered, the dynamical distortion (or CDW) will have a larger and larger coherence length until at T_c it becomes infinite and a static dimerization occurs in the stack. As all these changes affect the charge distribution around the N nuclei, the NQR spectrum therefore will reflect the changes in the CDW's produced by the Peierls transition. The narrow lines found in K-TCNQ showed the existence of commensurate (C) phases below 130 °C [see Figs. 4(a) and 4(b)] indicating that the CDW's are locked to the lattice at a C value. Above that temperature, the changes in the line shapes showed the existence of an incommensurate (IC) phase[15,25,26] and therefore of incommensurate CDW's. In the C phase, the number of resonance lines is determined by the small number of physically inequivalent nuclei present in the unit cell.[15,28] In IC phases, there is a continuous distribution of inequivalent sites and therefore a quasicontinuous distribution of the frequencies instead of the sharp lines observed in C phases.[15,28,29] In the IC phases, the resonance lines have a frequency distribution consisting of a broad background and distinct peaks (singularities). In the multisoliton limit, where walls and domains are present, a number of "commensurate" lines or "edges" exist in addition to the IC background and singularities as may be seen in Figs. 4(c)–4(h). When the C phase is reached, the IC background and singularities disappear and only the narrow C lines remain[15,28] as in Figs. 4(a)–4(d). The complex line shapes observed in K-TCNQ above 130 °C suggested that solitons were present above that temperature. The comparison between the observed lineshapes and those obtained by assuming a one-dimensional modulation wave with constant amplitude provided the best fit if a frequency distribution of the quadratic type was used.[15,28,29] The distribution employed was

$$f(\phi)=\text{const}/|\sin\phi\cos\phi|\{\Delta^2+\cos^2[p(\phi-\phi_0)]\}\ , \tag{1}$$

where p is the ratio of the unit-cell sizes at low and high temperature and ϕ is the phase of the modulation wave. The best fit was obtained with $p=2$ and Δ values of 0.005 and 0.010 with different initial phases for each HT site. The values of Δ showed that above 141.5 °C the line shapes observed corresponded to a multisoliton lattice[25,28] in the narrow soliton limit. On the other hand, the soliton density n_s may be obtained, if the values of Δ and ϕ_0 are known, from[28]

$$n_s=(\pi/2)/K[1/(1+\Delta^2)^{1/2}]\ , \tag{2}$$

where

$$K=\int_0^{\pi/2}d\psi[1/(1-k^2\sin^2\psi)^{1/2}]\ .$$

In this integral, $k=(1+\Delta^2)^{-1/2}$ and $\psi=p(\phi-\phi_0)$. For practical reasons K was approximated[30] as $K=(\pi/2)-\ln(1-k^2)$ and values of n_s of 0.25 and 0.23 were obtained from Eq. (2) for the two HT sites indicating that a noticeable soliton density existed above 141.5 °C. The CDW in the multisoliton lattice has an average wavelength that is incommensurate with the lattice, but locally the CDW has C regions separated by regions of phase slip that are called solitons or discommensurations.[25] In K-TCNQ these regions correspond to zones of fluctuating local dimerization of the stacks. The values of n_s found in this work showed that a considerable degree of dynamical dimerization exists above 141.5 °C in this salt. This result confirms the qualitative conclusions about the dynamical dimerization obtained from diffuse x-ray scattering measurement[4] and from ir polarized reflectivity spectra obtained in single crystals[3] of K-TCNQ.

C. The phase transition in K-TCNQ from NQR study

The complex set of transitions found in K-TCNQ starts from low temperature as continuous variations in the inter- and intradimer distances within the TCNQ stacks.[4] These changes produce a smooth variation in the resonance frequencies up to 128 °C. Between 128 and 130 °C, the narrow HT lines indicate that the CDW's may still be commensurate with the lattice, although their low intensity and the extensive superposition with the LT lines makes the detection of IC singularities difficult in this temperature range. Between 130 and 141.5 °C, the line shapes correspond to an IC phase that shows the depinning of the CDW's from the C values observed at lower temperatures. Just below 141 °C, the LT lines finally disappeared indicating that the first-order transition is completed at that temperature. At 141.5 °C, there is a noticeable change in the line shape that reflects a modification in the IC regime produced by the CDW's.

The s singularities always disappeared abruptly on cooling and appeared on heating at 141.5 °C while the HT lines were observable down to 90 °C. Such a behavior could be explained by assuming that the CDW's on cooling are locked with the lattice below 141.5 °C at a commensurate[3] value. On further cooling, the now commensurate HT structure is slowly transformed into the LT phase following the nucleation and growth mechanism typical of first-order transitions.[17] The appearance or disappearance of the s edges at 141.5 °C either on heating or on cooling suggests the existence of a second transition involving CDW's that was not detected previously.[1-5] The DSC results showed that on heating there is a noticeable heat absorption peak at that temperature in K-TCNQ. Furthermore, the small jump observed in the frequency of the b edge and the sudden variation in line shape at 141.5 °C also suggests the existence of that previously undetected second transition.[16] In this regard, Terauchi[4] found that the soft phonon frequency has an inflection point around 140 °C indicating a change in the interionic forces. This result suggests the presence of changes in the interstack (and CDW's) interactions that could reflect variations in the CDW's coherence length. It is known that the magnitude of the coherence length is strongly dependent on the effective dimensionality of the fluctuations.[27] Then, the variation in line shape observed at 141.5 °C may be attributed to a change in the effective dimensionality in the ordering of the CDW's along the stacks similar to that found[27] in TTF-TCNQ. As the temperature is raised above 141 °C, the s edges decreased steadily in intensity and about 10° below the decomposition point disappeared altogether. Then in the HT phase of K-TCNQ the narrow solitons found just above 141 °C on heating changed towards the single soliton limit[15,25] near the decomposition temperature. This change is the result of the expected decrease in the coherence length of the dynamical dimerization present along the $TCNQ^-$ stacks and the weakening of the electron- (or spin-) phonon interaction responsible for the Kohn anomaly.[27]

A comparison of the details of the Peierls transition found in TTF-TCNQ where the charge transfer[27] is around 0.6 and in fully ionic K-TCNQ shows that in both cases we have a similar set of successive complex transitions, with some of first-order and others related to ordering of the CDW's. Even in the so-called simple TCNQ salts such as K-TCNQ, the Peierls transition is a complex transformation that seems to involve several other factors beside the degree of charge transfer. Recently, Zhou and Gong[31] found theoretically that the Peierls transition should be a two-step process if the weak interstack couplings are properly taken into account. They found that the CDW transition should occur at a higher temperature than the metal- (or semiconductor-) insulator transition. The present NQR results seem to confirm this prediction as the dimerization connected with the gap opening occurs at lower temperatures than the CDW transition in K-TCNQ.

D. Temperature dependence of the NQR frequencies

The electric field gradients (EFG's) are averages over molecular motions[32] and the measured values of their components depend on the vibrational state of the molecule. In the gas phase, the molecular vibrational state is well defined and separate EFG values may be obtained for each vibrational energy level. In the solid state, it is the crystal lattice as a whole which is vibrating and only an average but temperature-dependent EFG is obtained.[32] Furthermore, in the solid a variety of intermolecular lattice vibrations and librations which contribute to the vibrational average of the EFG exist. The interval between the intermolecular levels is small, so that the vibrational amplitudes are noticeably temperature dependent. The vibrationally averaged EFG in the solid is then also temperature dependent and usually decreases its value as the temperature is increased[32] ($d\nu/dT<0$). In addition to the vibrational averaging, in the solid state the EFG's present in a molecule contain contributions arising from the neighboring atoms or molecules (crystal field) which are also vibrationally dependent. This last term, at least in complex ionic crystals, could be very important in determining the resulting thermal averaging of the EFG especially near temperatures where phase transitions occur.[11,32] Using the standard result for the average over vibrational states one obtains that the most important contribution to the EFG thermal averaging corresponds[32] to those modes with frequencies ω^j such that $\hbar\omega^j/kT\simeq 1$. Therefore the low-frequency inter- and intramolecular vibrations will determine the temperature dependence of the resonance lines.[32] In K-TCNQ, half of the ν^- lines showed an unusual positive $d\nu/dT$ value well below T_c that sharply increased on approaching the transition region. Additionally, two of the ν^+ lines exhibiting negative $d\nu/dT$ showed a decrease in their absolute values approaching T_c. These results indicate that the librational mechanism that produces negative and rather constant $d\nu/dT$ values is counteracted by the intra- and/or intermolecular contribution[11] below T_c. This conclusion is supported by the fact that immediately above that temperature only constant values were found for $d\nu/dT$ in both ν^+ and ν^- lines. As above T_c the librational averaging is also operative, then such a mechanism is not likely to produce the large changes observed in the $d\nu/dT$ values when T_c is approached from below.

In K-TCNQ there is also an interaction between the conduction electrons and intramolecular vibrations of proper symmetry that drives long-wavelength plasmalike electron oscillations in the range of intramolecular vibrational frequencies.[33-36] The electron-intramolecular vibration coupling is expected to be similar in all the CN groups due to the high molecular symmetry.[33-36] As only half of the N lines showed unusual $d\nu/dT$ values factors like the temperature dependence of low-frequency intramolecular vibrations or/and the changes in the crystal-field contribution to the EFG (Ref. 11) may be responsible for their behavior. The intramolecular contribution will be similar for all the N atoms due to the high molecular symmetry of TCNQ so the fact that only half of the lines have the unusual $d\nu/dT$ values points toward the changes in the crystal-field contribution as the main source of that behavior. The TCNQ stacks[5] change continuously with increasing temperature below T_c producing modifications in the average interionic distances.

Even small changes in these distances around a N nucleus will produce noticeable effects in the resonance frequencies because the EFG components depend exponentially upon the separation between ions that are in close contact.[37] In the LT phase at room temperature[5] there are two crystallographically inequivalent TCNQ stacks directed along the $\underline{a}$ axis with the molecular planes forming angles of 15.8° (stack I) and 11.3° (stack II), respectively, with the plane (100). In the HT phase[5] around 140 °C, only a single stack with an angle of 8.9° is found. Also, an increase in the intradimer distance and a decrease in the interdimer separation so to approach more closely a quasimonomeric structure is found in K-TCNQ as the temperature approaches[5] T_c. Nevertheless, the monomeric structure does not appear until T_c is attained.[4,5]

The inequivalence between columns suggest that the TCNQ molecules of stack I will change their orientation and interionic distances in a different way than the molecules of stack II in order to attain the quasimonomeric structure. Therefore lines of stacks I and II are expected to have a different temperature dependence especially near the transition point. By comparing the changes in structure with the changes in resonance frequencies with temperature it is possible to assign some lines to specific $TCNQ^-$ molecules. From Fig. 1 we see that on heating the frequency of the ν^+ lines *d*, *g*, *h*, and in a lesser degree the *a* line change toward the ν^+ line of higher frequency of the HT phase with a significant increase in the $d\nu/dT$ values on approaching T_c. The other ν^+ lines tend toward the frequency of the remaining HT ν^+ line with little change in their derivatives. Similarly, on heating the ν^- lines *h*, *g*, *f*, and *e* moved (as seen in Fig. 2) towards the ν^- line of highest frequency in the HT phase while the other four lines shifted towards the remaining ν^- line of that phase. It is easily seen that the N sites with the largest changes in the $d\nu/dT$ values should correspond to the LT sites whose spatial configuration differs most from those of the quasimonomeric structure as the stack I. Therefore, the lines with the largest changes in the derivatives may be assigned to the TCNQ ions of stack I of the LT phase.

The changes in the frequency with temperature are significantly more marked and start at much lower temperature[11] in the ν^- than in the ν^+ lines as seen in Figs. 1 and 2. As shown in Ref. 11, the ν^- line of a N atom in a CN group is linked with the population of the orbital which is perpendicular to the molecular plane ($\pi_\perp$) and which contains the extra electron in $TCNQ^-$. In turn, the ν^+ lines, which are connected to the population of the π orbital that is parallel to the molecular plane, are not affected by the extra electron. The larger sensitivity of the ν^- lines to the effects of the transition is then related to the much higher polarizability of the $\pi_\perp$ orbital[11] containing the extra electron and to the variations produced in the population of that orbital by the modifications with temperature of the overlap between molecules of the same stack.[5]

In conclusion, it is clear that the Peierls (or spin-Peierls) transition observed in K-TCNQ is far more complex than previously assumed for fully ionic and simple salts of TCNQ and shows a noticeable similarity with that found in TTF-TCNQ. This result indicates the Peierls (or the spin-Peierls) transition is probably a complex two-step process as predicted by Zhou and Gong.[31]

APPENDIX: CORRECTIONS TO THE LINE INTENSITIES

The basic assumption in the corrections for the dependence on experimental parameters (dispersion) of the line intensity or amplitude response of the spectrometer is the independence of three instrumental effects, which are necessarily variable from one measurement to another, namely, (1) the difference between the irradiation and observation frequencies (offset), (2) the selectivity of the resonant parallel LC circuits in both the receiver and sample network, (3) the dependence of the receiver gain on the absolute working frequency, beyond that introduced by the internal resonant circuits. The independence of these three parameters, means that the measured amplitude[14] (A) is

$$A = A_0 M_0 M_s M_g \ ,$$

where A_0 is the idealized amplitude response of the spectrometer, M_0 is the offset, M_s is the selectivity, while M_g is the receiver gain. These parameters will be a function of four frequencies: (1) the resonance frequency of the absorption line, F_0; (2) the frequency of the transmitter, F_f; (3) the tuning frequency of both sample and receiver LC circuits, F_t; (4) a frequency conveniently chosen as a reference for the gain of the receiver, F_r. Then M_0 will be $F_t - F_0$, while M_s will be a function of the detuning, $D = (F_0 - F_t)/F_t$; and M_g of the offset from the reference frequency.

(1) The dependence of F_0 contains two effects: (a) the frequency distribution of the magnetic rf field generated by the pulse, which is the Fourier transform of the pulse envelope; (b) the response of a system of spin $=1$ nuclei to a pulsed magnetic field of given intensity. As far as effect (a) is concerned, one has that if the pulse envelope has infinitely short rise and fall times, and duration T_p, the frequency distribution of its amplitude (hence its effective flip angle) will be proportional to $\sin(x)/x$ where $x = F_0 T_p$. The relationship between the effective flip angle and $\sin(x)/x$ involves the determination of several parameters of difficult measurement so a more practical approach was attempted. That approach used the duration of the pulse giving the maximum NQR signal at $F_0 = 0$ is called T_m or "90° pulse." Then the effective flip angle A is

$$A = (T_p/T_m)\,2.076\,94\,|\sin(F_0 T_p)/F_0 T_p| \ .$$

The absolute value is required because we actually measure an absolute value spectrum.

The values of M_0 are given by

$$M_0 = (1/0.436\,179)[\sin(A) - A\cos(A)]/(A^2) \ .$$

The numeric factor is necessary in order to have $M_0 = 1$ when a 90° pulse is applied. The value of T_p was obtained from a fitting of a series of measurements of the amplitude of a line as a function of F_0. In order to obtain a

good fitting, around 70 spectra were taken with F_0 ranging from -120 to $+70$ kHz. These values of F_0 are much larger than those used in the actual measurements ($+40$ kHz). In order to avoid complications arising from the line overlap, the two-line spectrum obtained on cooling from 190 °C at 140 °C in K-TCNQ was used for all the measurements. The tuning circuits were set at a value that was kept constant throughout the measurements, since the observation frequency was actually the same for all the measurements in this series.

(2) If the overall selectivity of the receiver and sample circuits may be described as that of a single parallel resonant circuit having a quality factor Q, then the M_s may be obtained from the universal resonance curve.[37] This curve was used in a fitting procedure to data gathered by injecting into the input of the receiver a small rf signal of the frequency synthesizer that was amplitude modulated at low frequency. The sample circuit was left at the input of the receiver and the low-frequency output of the receiver was measured against the carrier frequency. Although the parameter of interest here was Q, F_t was also refined, since its exact value affects that of Q. Furthermore, since the observation frequency was variable, the measured output was corrected, before fitting, for the frequency dependence of the receiver's gain.

(3) The dispersion of the gain of the receiver was taken into account on a purely empirical basis: the experimental gain and frequency values were found to fall in a straight line, whose parameters were used to compute M_g. The experimental points were gathered exactly as in (2); this time, however, both the receiver and sample circuits were retuned accurately each time the frequency of the synthesizer was changed.

In each of the fittings described so far, an auxiliary fitting parameter had to be added, which was the "best chosen" scale factor for reducing the arbitrarily scaled amplitudes to relative values, i.e., to unit amplitude when no correction is needed.

---

*To whom the correspondence should be addressed.

[1]J. G. Vegter, T. Hibma, and J. Kommandeur, Chem. Lett. **3**, 427 (1969); T. Hibma and J. Kommandeur, Phys. Rev. B **12**, 2608 (1975).

[2]M. Sakai, I. Shirotani, and S. Minomura, Bull. Chem. Soc. Jpn. **45**, 3314 (1972).

[3]H. Okamoto, Y. Tokura, and T. Koda, Phys. Rev. B **36**, 3858 (1987).

[4]H. Terauchi, Phys. Rev. B **17**, 2446 (1978).

[5]M. Konno, T. Ishii, and Y. Saito, Acta Cryst. **B33**, 763 (1977).

[6]R. Bozio and C. Pecile, J. Chem. Phys. **67**, 3864 (1977).

[7]R. Bozio and C. Pecile, *The Physics and Chemistry of Low-Dimensional Solids,* edited by L. Alcacer (Reidel, Amsterdam, 1980).

[8]Y. Lepine, A. Caille, and V. Larochelle, Phys. Rev. B **18**, 3835 (1978).

[9]Y. Takaoka and K. Motisuki, J. Phys. Soc. Jpn. **47**, 1752 (1979).

[10]T. P. Das and E. L. Hahn, *Nuclear Quadrupole Resonance Spectroscopy* (Academic, New York, 1958).

[11]J. Murgich, J. Chem. Phys. **70**, 5354 (1979).

[12]L. R. Melby, R. J. Harder, W. R. Hertler, R. E. Benson, and W. E. Mochel, J. Am. Chem. Soc. **84**, 3374 (1962).

[13]R. Ambrosetti, R. Angelone, A. Colligiani, and A. Rigamonti, Phys. Rev. B **15**, 4318 (1977).

[14]A. Colligiani and R. Ambrosetti, Gazz. Chim. Ital. **106**, 439 (1976).

[15]R. Blinc, Phys. Rep. **79**, 331 (1981).

[16]R. L. Armstrong and H. M. van Driel, Adv. Nucl. Quad. Res. Spectrosc. **2**, 179 (1975).

[17]Yu. V. Mnyukh, Mol. Cryst. Liq. Cryst. **52**, 163 (1979).

[18]G. Byrne, *Recovery, Recrystallization and Grain Growth* (Macmillan, New York, 1965).

[19]M. H. Cohen and F. Reif, *Solid State Physics,* edited by F. Seitz and D. Turnbull, (Academic, New York, 1957), Vol. 5, p. 352.

[20]J. L. Goudard, A. A. Lakhani, and N. K. Hota, Solid State Commun. **41**, 423 (1982).

[21]V. J. Emery, in *Chemistry and Physics of One-Dimensional Metals,* edited by H. J. Keller (Plenum, New York, 1977).

[22]R. F. Peierls, *Quantum Theory of Solids* (Oxford University Press, Oxford 1955).

[23]I. S. Jacobs, J. W. Bray, H. R. Hart, Jr., L. V. Interrante, J. S. Kasper, G. D. Watkins, D. E. Prober, and J. C. Bonner, Phys. Rev. B **14**, 3036 (1976).

[24]S. K. Khanna, A. A. Bright, A. F. Garito, and A. J. Heeger, Phys. Rev. B **10**, 2139 (1974).

[25]W. L. McMillan, Phys. Rev. B **12**, 1185 (1975); **14**, 1496 (1976).

[26]B. H. Suits, S. Couturie, and C. P. Slichter, Phys. Rev. Lett. **45**, 194 (1980).

[27]A. J. Heeger, in *Chemistry and Physics of One-Dimensional Metals,* edited by H. J. Keller (Plenum, New York, 1977).

[28]R. Blinc, O. Prelovsek, V. Rutar, J. Seliger, and S. Zumer, in *Incommensurate Phases in Dielectrics,* edited by R. Blinc and A. P. Levanyuk (North-Holland, Amsterdam, 1986), Vol. 1, p. 144.

[29]J. Murgich, Phys. Rev. B **35**, 3563 (1987).

[30]A. Colligiani, C. Pinzino, and R. Angelone, Mol. Phys. **62**, 97 (1987).

[31]C. Zhou and C. Gong, J. Phys. C **21**, L561 (1988).

[32]E. A. C. Lucken, Adv. Nucl. Quad. Res. Spectrosc. **5**, 83 (1983).

[33]M. J. Rice, N. O. Lipari, and S. Strassler, Phys. Rev. Lett. **39**, 1359 (1977); C. B. Duke, Ann. N.Y. Acad. Sci. **313**, 166 (1977).

[34]C. Carlone, C. Cyr, S. Jandl, N. K. Hota, and J. Zauhar, J. Chem. Phys. **77**, 4920 (1982).

[35]B. Lunelli and C. Pecile, J. Chem. Phys. **52**, 2375 (1970); R. Bozio and C. Pecile, *ibid.* **67**, 3864 (1977).

[36]T. B. Brill, J. Chem. Phys. **61**, 424 (1974).

[37]F. E. Terman, *Electronic and Radio Engineering* (McGraw-Hill, New York, 1955).